Improving functionality of vibration energy harvesters using magnets

Tang, Lihua; Yang, Yaowen; Soh, Chee Kiong

2012

Tang, L., Yang, Y., & Soh, C. K. (2012). Improving functionality of vibration energy harvesters using magnets. Journal of Intelligent Material Systems and Structures, 23(13), 1433-1449.

https://hdl.handle.net/10356/83695

https://doi.org/10.1177/1045389X12443016

Improving Functionality of Vibration Energy Harvesters Using Magnets

Lihua TANG [1], Yaowen YANG [2]* and Chee-Kiong SOH [3]

[1,2,3] School of Civil and Environmental Engineering,

Nanyang Technological University, 50 Nanyang Avenue, Singapore 639798

*Corresponding author, cywyang@ntu.edu.sg

ABSTRACT

In recent years, several strategies have been proposed to improve the functionality of energy harvesters under broadband vibrations, but they only improve the efficiency of energy harvesting under limited conditions. In this work, a comprehensive experimental study is conducted to investigate the use of magnets for improving the functionality of energy harvesters under various vibration scenarios. Firstly, the nonlinearities introduced by magnets are exploited to improve the performance of vibration energy harvesting. Both monostable and bistable configurations are investigated under sinusoidal and random vibrations with various excitation levels. The optimal nonlinear configuration (in terms of distance between magnets) is determined to be near the monostable-to-bistable transition region. Results show that both monostable and bistable nonlinear configurations can significantly outperform the linear harvester near this transition region. Secondly, for ultra-low-frequency

vibration scenarios such as wave heave motions, a frequency up-conversion mechanism using magnets is proposed. By parametric study, the repulsive configuration of magnets is found preferable in the frequency up-conversion technique, which is efficient and insensitive to various wave conditions when the magnets are placed sufficiently close. These findings could serve as useful design guidelines when nonlinearity or frequency up-conversion techniques are employed to improve the functionality of vibration energy harvesters.

Keywords: energy harvesting, piezoelectric, vibration, magnets, nonlinearity, frequency up-conversion

1 INTRODUCTION

The continuous reduction in power consumption of wireless sensing electronics has evoked the possibility to implement self-powered sensors via harvesting the ambient vibration energy. In the past few years, considerable research efforts have been devoted to improving the efficiency of vibration energy harvesters (Anton and Sodano, 2007; Tang et al., 2010, 2011). Vibrations can be converted into electricity via electromagnetic (El-Hami et al., 2001), electrostatic (Roundy et al., 2003), piezoelectric (Yang et al., 2009; Yang and Tang, 2009) and magnetostrictive (Wang and Yuan, 2008) mechanisms. Regardless of the mechanism adopted, most of the vibration energy harvesters reported in the literature have been designed as linear mechanical resonators that can only effectively collect energy within a narrow

bandwidth. With a slight drift from the resonance, their performances will decrease drastically. Even though the geometric and physical properties of a harvester can be carefully selected for frequency matching, unfortunately, the frequencies of vibration sources usually vary in a certain range. In some scenarios, such as human movements and wave heave motions, it is not feasible to match the frequency of harvester with the vibration source as it is too low. Actually, it is meaningless to harvest energy at such ultra-low frequencies. Therefore, frequency up-conversion techniques are necessary for such scenarios. Moreover, the vibrations in majority of practical cases are presented in random patterns, causing much difficulty in designing the harvesters. To address the above issues, the key is to improve the functionality of energy harvesters for various vibration scenarios, which is the objective of this study.

To design a system incorporating certain resonance tuning mechanism was the first approach realized by researchers. Applying mechanical preload (Leland and Wright, 2006; Hu et al., 2007) and using magnetic forces (Challa et al., 2008, 2011) and piezoelectric actuators (Peters et al., 2009; Wischke et al., 2010) have been widely adopted as the tuning mechanisms. However, the complexity of implementing automatic tuning and the energy consumption for the control circuit are critical issues to be addressed.

In very recent years, exploiting the nonlinearities has become an optional solution for broadband energy harvesting. Mann and Sims (2009) presented a design for

electromagnetic energy harvesting from the nonlinear oscillations of magnetic levitation. Ramlan et al. (2010) investigated the hardening mechanism of a monostable nonlinear energy harvester via analytical and numerical studies. Stanton et al. (2009) proposed a monostable harvester in which both the hardening and softening responses could occur by tuning the magnetic interactions. Since the response curve was bent in the monostable configurations, large-amplitude oscillations would persist over a much wider frequency range. Besides, a larger output could be obtained by the monostable harvester as compared to the linear configuration. However, the wider bandwidth and improved performance of monostable harvesters can only be achieved conditionally. Daqaq (2010) claimed that, under white or colored Gaussian excitation environment, the hardening-type nonlinearity failed to improve and even reduced the output power as compared to the typical linear harvesters. Other than monostable configurations, bistable nonlinear harvesters are also widely reported in the literature. Erturk et al. (2009) investigated the bistable mechanism of a broadband piezo-magneto-elastic generator under sinusoidal excitations. Cottone et al. (2009) implemented a piezoelectric inverted pendulum using the bistable configuration under stochastic excitations. Ferrari et al. (2010), Lin and Alphenaar (2010), Andò et al. (2010) and Stanton et al. (2010) extended this idea to study the energy harvesting performance of bistable cantilevers with repulsive magnets under wide-spectrum vibrations. McInnes et al. (2008) and Formosa et al. (2009) proposed to enhance the performance of a bistable system for energy harvesting by exploiting the phenomenon of stochastic resonance, which occurs if the potential barrier of a dynamic system is

appropriately forced to oscillate.

In ultra-low-frequency scenarios, frequency up-conversion techniques have been pursued as an alternative frequency-robust solution for vibration energy harvesting. Rastegar et al. (2006) presented a two-stage concept in which the low-frequency vibrations of a primary unit were transferred to high-frequency vibrations of the secondary vibration units, i.e., cantilevered piezoelectric generators. To avoid mechanical impact loss, attractive magnetic forces either by pairs of magnets (Rastegar and Murray, 2009) or by ferromagnetic structures (Wickenheiser and Garcia, 2010), were utilized to induce impulses to the cantilevered energy harvesters. However, repulsive magnetic configuration has not been reported in the literature for such frequency up-conversion devices.

This paper presents a comprehensive experimental study on the use of magnets to improve the functionality of energy harvesters under various vibration scenarios. Firstly, nonlinearities introduced by the magnets are exploited to improve the performance of energy harvesting. Both monostable and bistable configurations are investigated under sinusoidal and random vibrations with various excitation levels. The nonlinear energy harvester is demonstrated to be able to outperform its linear counterpart except for the monostable softening configuration and the bistable configuration with too closely placed magnets. Under practical random vibrations, the optimal nonlinear configuration is found near the monostable-to-bistable transition

region. Moreover, it is observed that the performance enhancement of nonlinear configurations is attributed to two aspects: the increased output magnitude in the frequency domain for low-level excitations and the enlarged bandwidth for high-level excitations. Secondly, for ultra-low-frequency scenarios such as wave heave motions, a frequency up-conversion mechanism using magnets is proposed. Different configurations under various wave conditions are investigated by parametric study. The repulsive configuration of magnets is found to be favorable in the frequency up-conversion technique, and its capability can be saturated and insensitive to wave conditions when the magnets are placed sufficiently close. The findings presented in this paper provide useful guidelines when one seeks nonlinearity or frequency up-conversion techniques using magnets to improve the functionality of vibration energy harvesters.

2 EXPLOITING NONLINEARITIES USING MAGNETS

At the very beginning when permanent magnets were used in energy harvesting devices, they played the role of vibration-to-electricity transduction obeying Faraday's law. Later, in order to enable the energy harvesters to adapt in frequency-variable circumstances, magnetic forces were introduced to tune the structural resonance of the energy harvesters (Challa et al., 2008). The resonance tuning mechanism using magnets is briefly described here. A typical resonance-tunable energy harvester and the layout of experiment apparatus are shown in Figure 1. Two piezoelectric transducers are bonded at the root of a cantilevered aluminum beam to form a

bimorph harvester. Two NdFeB permanent magnets with diameter of 10mm, thickness of 5mm and surface flux of 3500 gauss are held in plastic holders and spanned at a distance D. With the arrangement of attractive or repulsive magnets at various distances, the stiffness of the bimorph cantilever can be altered accordingly and thus its resonance frequency tuned.

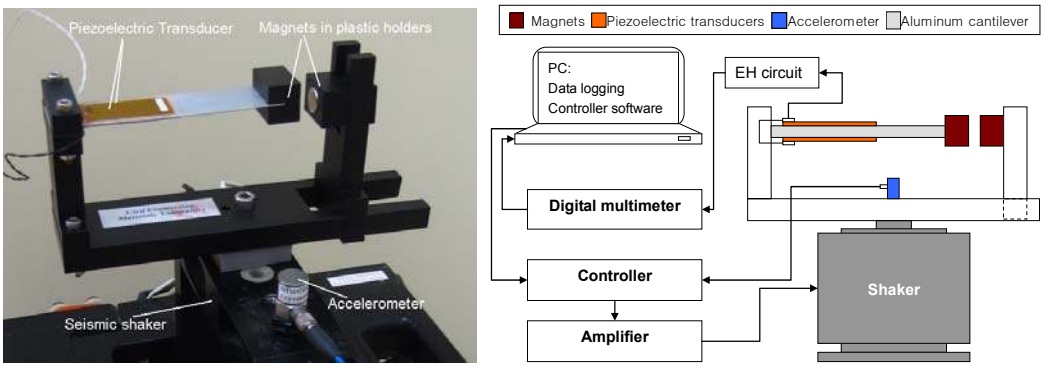

(a) (b)

Figure 1 (a) Resonance-tunable energy harvester and (b) Layout of experiment apparatus

The sweep responses of open circuit voltage V_{OC} under low-level sinusoidal excitations (a_{RMS} = 0.2~0.5m/s^2) are shown in Figure 2. The resonance can be tuned bi-directionally with repulsive or attractive magnets. It should be mentioned that the off-resonance responses of some configurations are quite small. Hence, different excitation levels are applied for different configurations to ensure accurate data reading and V_{OC} in Figure 2 are normalized by acceleration. Besides, it is noted in Figure 2 that the harvester coupled with magnetic forces still behaves like a linear one under low-level excitations.

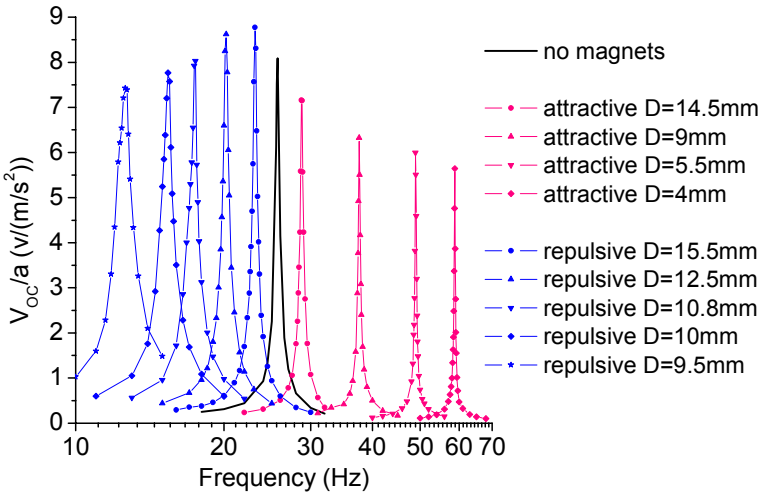

Figure 2 Resonance tuning under low-level excitations

Here the resonance is manually tuned. Although the feedback-loop control has been successfully implemented for automatic tuning as reported by Challa et al. (2011), the huge energy consumption for actuators requires the harvester to accumulate enough energy for a long time before starting one tuning process, which is unfeasible if the excitations vary from time to time or present in the form of random vibrations. Hence, it is preferable if broadband energy harvesting can be achieved in a passive mode (no extra energy injection is required).

With the increase of excitation level, nonlinear behaviors will appear. The experiment setup for the nonlinear harvester is the same as that shown in Figure 1. The system can be modeled as a nonlinear pendulum with dipole-dipole magnetic interaction. The potential energy of the system can be expressed as follows (Cottone et al., 2009; Andò et al., 2010):

$$U(x)=\frac{1}{2}K_0x^2+\frac{\mu_0 m_1 m_2}{2\pi d}\left(d^2x^2+\mathrm{D}^2\right)^{-\frac{3}{2}} \tag{1}$$

where x represents the deflection of the harvester; K_0 (K_0>0) is the effective stiffness of the initial linear configuration (without magnetic interaction); $\mu_0=4\pi\times10^{-7}\mathrm{NA}^{-2}$ is the permeability constant; m_1 and m_2 are the effective magnetic moments; d is a geometrical parameter related to the point of measuring the displacement x and the cantilever length; and D is the distance between the two magnets. For the prototype in our experiment, d=1, m_1=m_2=m=0.2Am^2 for repulsive arrangement, m_1=-m_2=m=0.2Am^2 for attractive arrangement and K_0=226Nm^{-1} (calculated from the static deflection due to a concentrated transverse force at the free end of the cantilever beam by finite element analysis). Thus, the potential energy for different magnet configurations is shown in Figure 3.

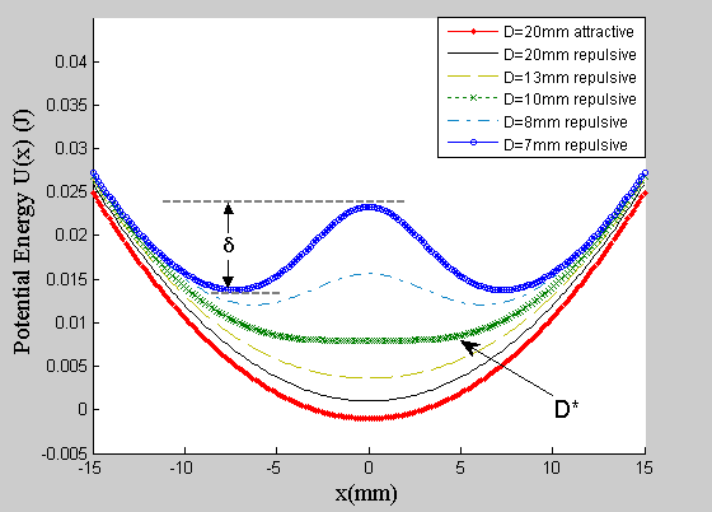

Figure 3 Theoretical prediction of potential energy $U(x)$ for different magnet configurations

To further understand the nonlinearity introduced by the magnets, we expand the

second term in Eq. (1) as a Maclaurin series,

$$\frac{\mu_0 m_1 m_2}{2\pi d}\left(d^2x^2+\mathrm{D}^2\right)^{-\frac{3}{2}}=\frac{\mu_0 m_1 m_2}{2\pi d}\left(\mathrm{D}^{-3}-\frac{3}{2}d^2\mathrm{D}^{-5}x^2+\frac{15}{8}d^4\mathrm{D}^{-7}x^4\right)+\mathrm{O}\left(x^4\right) \tag{2}$$

Ignoring the high-order terms, the potential energy function can be approximated as

$$U(x)\approx\frac{1}{2}(K_0+K_1)x^2+\frac{1}{4}ax^4+C \tag{3}$$

where

$$K_1=-\left(\frac{\mu_0 m_1 m_2}{2\pi}3d\mathrm{D}^{-5}\right),\quad a=\frac{\mu_0 m_1 m_2}{2\pi}\frac{15}{2}d^3\mathrm{D}^{-7},\quad C=\frac{\mu_0 m_1 m_2}{2\pi d}\mathrm{D}^{-3} \tag{4}$$

and the spring force of the system can be approximated as

$$F(x)\approx(K_0+K_1)x+ax^3 \tag{5}$$

where K_1x and ax^3 are the linear and nonlinear components of the spring force introduced by the magnets, respectively. For the two attractive magnets, we have $K_1=\left(\mu_0 m^2/2\pi\right)3d\mathrm{D}^{-5}>0$ and $a=-\left(\mu_0 m^2/2\pi\right)\frac{15}{2}d^3\mathrm{D}^{-7}<0$, that is, the linear part of the magnetic force stiffens the harvester but the cubic nonlinear part induces a "softening" nonlinear behavior. While for two repulsive magnets, we have $K_1=-\left(\mu_0 m^2/2\pi\right)3d\mathrm{D}^{-5}<0$ and $a=\left(\mu_0 m^2/2\pi\right)\frac{15}{2}d^3\mathrm{D}^{-7}>0$. For a large D, $K_0+K_1>0$ still holds, thus the harvester has a reduced linear stiffness and a "hardening" nonlinear behavior. In these cases, only one stable equilibrium exists at $x=0$ in the potential energy (Figure 3). Hence, the configuration providing softening or hardening behavior is termed "monostable configuration". To avoid any confusion, from here onwards in this paper, "softening" and "hardening" refer to the nonlinear behavior of the harvester rather than the change in linear stiffness. This is consistent with the definition given in the literature (Ferrari et al., 2010; Stanton et al., 2009; Ramlan et al., 2010). When D decreases and passes a critical value, negative linear stiffness

(K_0+K_1<0) appears, resulting in two stable equilibriums in the potential energy, separated by the unstable equilibrium at x=0 (Figure 3). Such nonlinear configuration is termed "bistable configuration". By letting K_0+K_1=0, this critical distance between two repulsive magnets D* can be expresses as $D^* = \left(3d\mu_0 m^2 / 2\pi K_0\right)^{\frac{1}{5}}$. Using the parameters given previously, the theoretical value of D* is obtained as ≈10mm for the prototype in our experiment. While in the experiment, D* is achieved around 9.0 to 9.5 mm. The discrepancy between the theoretical and experimental values may result from the assumption of dipoles for magnets.

2.1 Monostable Configuration

This section discusses the nonlinear softening and hardening responses introduced by magnets. It can achieve broadband energy harvesting in a totally passive mode, different from the active resonance tuning method. Tests under both sinusoidal and random excitations are performed.

2.1.1 Monostable Configuration under Sinusoidal Excitations

The voltage outputs for a monostable hardening configuration (repulsive magnets with a gap D=9.5mm) and a monostable softening configuration (attractive magnets with a gap D=7.5mm) under three sinusoidal excitation levels are illustrated in Figure 4. Both upward and downward sinusoidal sweeps are conducted for each nonlinear case and compared with that from the linear configuration.

In the monostable hardening case (Figure 4(a)), for low-level excitation (a_{RMS}=0.5m/s^2) and thus small response *x*, the nonlinear part of the spring force induced by magnets (Eq. (5)) is negligible. Only the linear part affects the behavior of harvester, which can be used for resonance tuning (Figure 2). Hence, the peak of response curve is slightly shifted (i.e., the harvester behaves like a linear one) and the upward and downward sweeps do not create remarkable difference in responses (top of Figure 4(a)). With the increase of excitations to a_{RMS}=1.4m/s^2 (bottom of Figure 4(a)), the response curve is significantly bent to right, providing useful voltage output up to 15Hz by upward sweep. After 15Hz, the harvester cannot maintain the large-amplitude oscillations and suddenly jumps to the stable low-energy orbit. At the same excitation level (a_{RMS}=1.4m/s^2), by downward sweep, the monostable hardening harvester can re-capture the high-energy orbit at 14Hz. In other words, between 14Hz to 15Hz, high-energy and low-energy orbits co-exist. The high energy orbit is unstable, and can only be captured by upward sweep (or by some disturbance).

In the monostable softening case (Figure 4(b)), similar to the hardening case, no difference is observed between upward and downward sweep for low-level excitations, and the response curves are slightly bent. With the increase of excitation level to a_{RMS}=1.4m/s^2, opposite to the hardening case, the peak of response curve shifts to the left and can reach as far as 40Hz by downward sweep. The upward sweep can re-capture the large-amplitude oscillations at around 40.5Hz. Hence 40 to 40.5Hz is the range where high-energy and low-energy orbits co-exist.

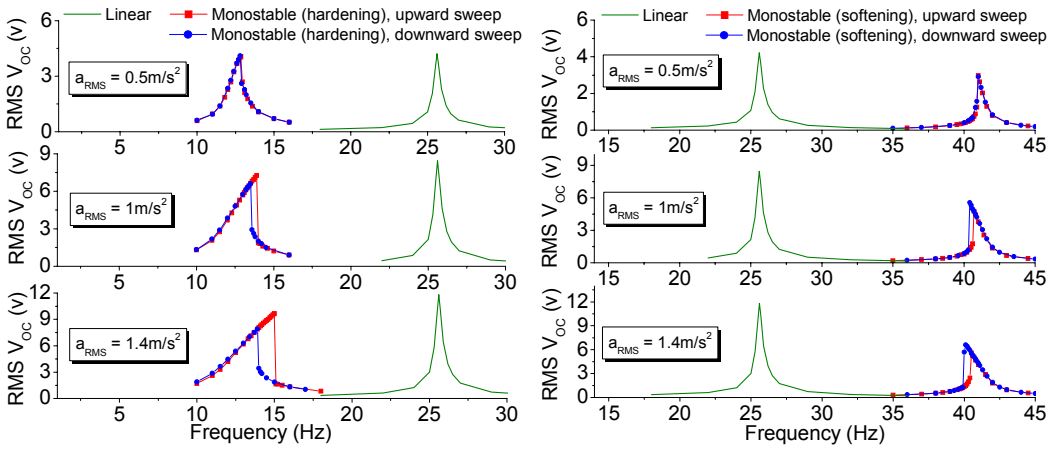

(a) (b)

Figure 4 Sinusoidal sweep responses of monostable configurations versus linear configuration for various excitation levels: (a) monostable hardening case (D=9.5mm); (b) monostable softening case (D=7.5mm)

Obviously, since the response curves of monostable configurations are bent with the increase of excitation level, useful voltage output covers wider frequency ranges as compared to a linear configuration. For example, at the voltage level of 3V under a_{RMS}=1.4m/s^2, the monostable hardening configuration by upward sweep provides a bandwidth of 11.2Hz~15Hz, while the linear configuration only provides a bandwidth of 25Hz~26.3Hz (bottom of Figure 4(a)). However, in terms of the magnitude of output under sinusoidal excitation, both hardening and softening configurations show no superiority to the linear configuration. Moreover, the wider bandwidth of a monostable harvester must be achieved with proper sinusoidal sweep. Hence, it cannot be concluded from the results of sinusoidal excitations that a monostable configuration can outperform its linear counterpart. Further study on its performance

under random excitations is needed, and is presented in the next section.

2.1.2 Monostable Configuration under Random Excitations

The majority of the vibration sources in our daily life presents in random patterns with energy distributed mostly in low frequency range (<200Hz) and with a relatively flat acceleration spectrum (Roundy et al., 2003). In this section, the acceleration amplitude of random excitations is assumed to be uniformly distributed over a bandwidth of 7Hz~100Hz, as shown in Figure 5. Such profile is close to the vibration spectra for office windows next to a busy street (refers to Figure 2 in Roundy et al. (2003)). The efficiencies of different monostable configurations are investigated at three random excitation levels, namely, a_{RMS}=2.5m/s^2, 5m/s^2 and 10m/s^2.

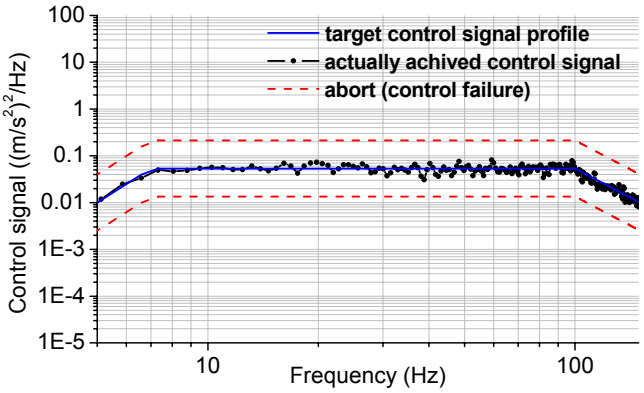

Figure 5 A sample of random control signal input in shaker controller (a_{RMS}=2.5m/s^2)

Figure 6 compares the open circuit voltage V_{OC} in time domain from various monostable configurations and linear harvester. The responses of the softening configuration (attractive magnets) are observed to be always smaller than those of the linear configuration at various excitation levels. On the other hand, the responses of

hardening configurations can be significantly larger than that of the linear harvester, especially when the magnets is closely placed (D=9.5mm).

The energy storage circuit is also considered here to evaluate from another perspective the energy harvesting performance of different configurations. Rectifying the output from the harvester by an AC/DC full-wave bridge and charging a storage capacitor of 33μF, the voltages developed across the capacitor for various configurations and excitation levels are compared in Figure 7. The time duration of charging is set to be sufficiently long (45 seconds) to ensure that the ultimate voltage developed across the storage capacitor under random excitations is nearly repeatable. From here onwards, we refer to charging the 33μF capacitor for 45 seconds when considering the energy storage circuit. In Figure 7, the softening configuration is found to be unable to outperform the linear configuration while the monostable configurations successfully outperform the linear configuration. For the hardening configuration with repulsive magnets arranged closely (D=9.5mm), the capacitor is charged fastest among the four configurations. If the magnet span is larger (D=10.5mm), the hardening configuration has no substantial advantage over the linear configuration under large excitation level, as shown in Figure 7(c). These conclusions drawn from Figure 7 are consistent with the observations of V_{OC} responses in Figure 6.

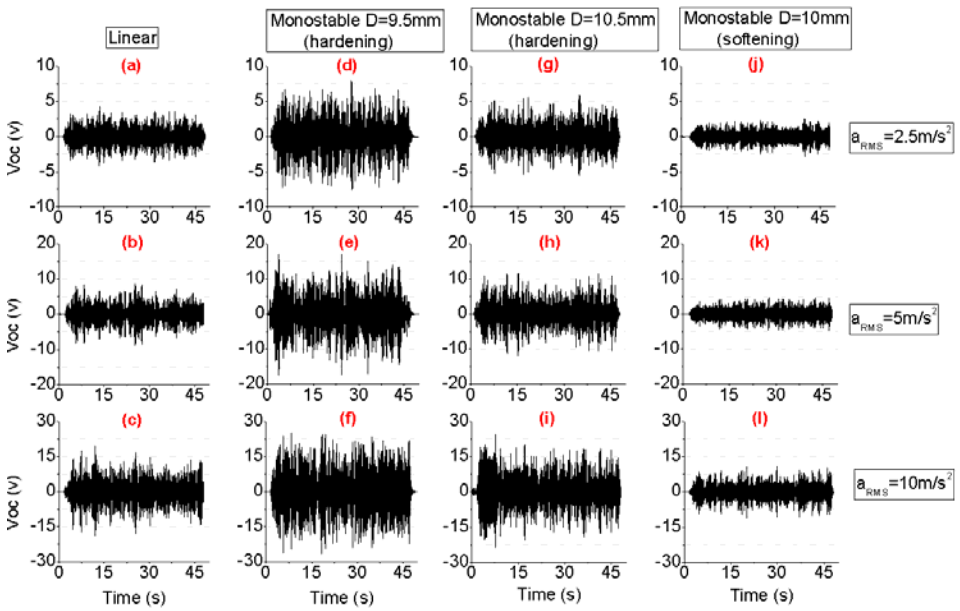

Figure 6 V_{OC} of linear and monostable configurations under random excitations

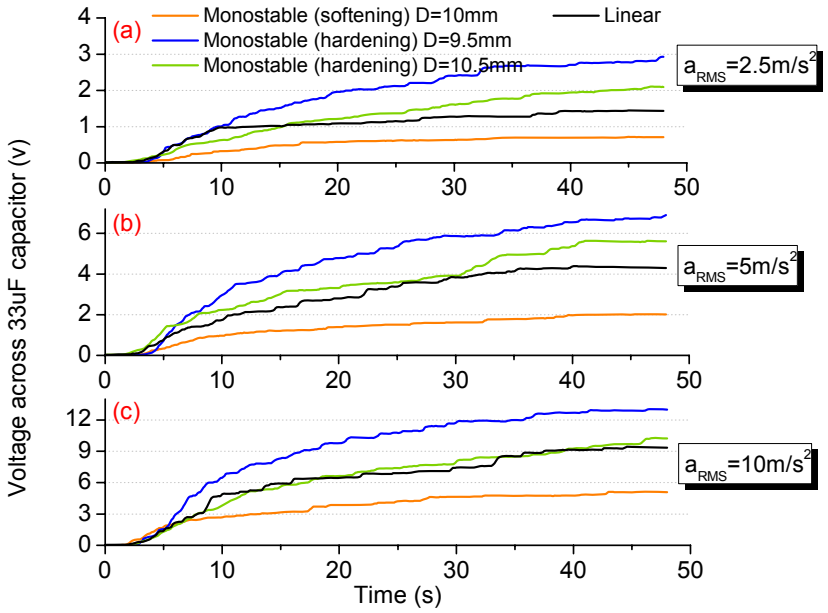

Figure 7 Voltage developed across storage capacitor for linear and monostable configurations under random excitations

To investigate the bandwidth of monostable configuration, fast Fourier transform

(FFT) is conducted and the V_{OC} spectra of different configurations are shown in Figure 8. From Figure 8, we can explain why the hardening configuration (especially for D=9.5mm) can outperform its linear counterpart. Applying the Plancherel theorem (Bracewell, 1978),

$$\int_0^{+\infty} \left|V_{OC}(t)\right|^2 dt = \int_0^{+\infty} \left|\hat{V}_{OC}(\omega)\right|^2 d\omega \tag{6}$$

the Fourier transform preserves the energy of the original quantity. Under low-level excitations, the hardening configuration has no obvious wider bandwidth than the linear configuration, but the larger magnitude is achieved in the frequency domain (Figure 8(a)), which means that $\int_0^{+\infty} \left|\hat{V}_{OC}(\omega)\right|^2 d\omega$ for the hardening configuration is larger than that for the linear configuration. Hence, according to the Plancherel theorem, it is no surprise that the hardening configuration has a larger $\int_0^{+\infty} \left|V_{OC}(t)\right|^2 dt$ and thus larger magnitude of V_{OC} in the time domain (comparing Figures 6(d) and 6(a)). Under high-level excitations, the hardening configuration (especially for D=9.5mm) has no obvious larger magnitude in the frequency domain, but the wider bandwidth is observed (Figure 8(c)). This also means that $\int_0^{+\infty} \left|\hat{V}_{OC}(\omega)\right|^2 d\omega$ for the hardening configuration is larger than that of the linear configuration, and thus a larger $\int_0^{+\infty} \left|V_{OC}(t)\right|^2 dt$ and V_{OC} magnitude in the time domain (comparing Figures 6(f) and 6(c)). Finally, the higher magnitude of V_{OC} in the time domain contributes to the higher energy harvesting rate when charging the capacitor (Figure 7(c)).

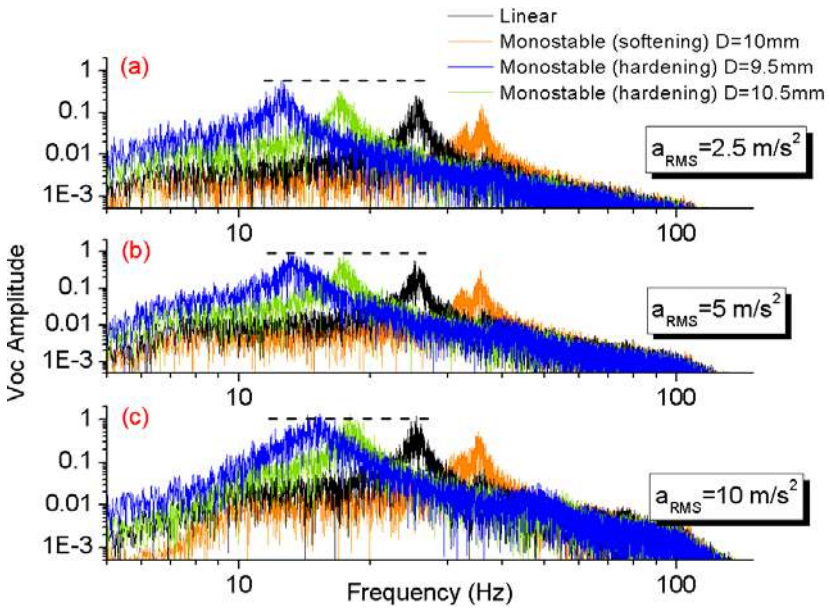

Figure 8 V_{OC} spectra (FFT) of linear and monostable configurations under random excitations

2.1.3 Summary of Monostable Configuration

Monostable nonlinear energy harvester can be implemented by using twin repulsive or attractive magnets. Under low-level sinusoidal excitations, the nonlinear part of the magnetic force is negligible while the linear part causes the change of linear stiffness of the harvester that can be used for resonance tuning. Under high-level sinusoidal excitations, high-energy and low-energy orbits co-exist in certain frequency range. Wider bandwidth for energy harvesting can be achieved by proper sweep or by disturbance, especially for the hardening configuration. Under practical broadband random excitations, monostable hardening configuration is demonstrated to be able to significantly outperform the linear configuration, especially when the repulsive magnets are closely placed (D=9.5mm). The improved performance can be attributed

to two aspects: the increased output magnitude in the frequency domain under low-level excitations and the enlarged bandwidth under high-level excitations.

2.2 Bistable Configuration

The experiment setup for bistable configuration is the same as that for the monostable hardening configuration. By decreasing the gap D between the repulsive magnets to a certain threshold D*, negative linear stiffness ($K_1+K_0<0$) and double stable equilibriums appear as shown in Figure 3. That is, by reducing the gap D, the harvester can move from a monostable configuration to a bistable one. If the harvester can oscillate between the two stable equilibriums under specific excitations, the voltage output can be remarkably improved. With the decrease of D, the two potential wells can be separated further, which intuitively can further help improve the performance of bistable configuration. However, the decrease of D also increases the energy barrier δ between the two potential wells as shown in Figure 3, causing difficulty for the harvester to jump between the two equilibrium states. Hence, reducing the gap D enables the harvester to reach a bistable configuration but does not guarantee its performance improvement if D is further reduced. In this section, various bistable configurations are investigated and compared with the linear counterpart under different levels of sinusoidal and random excitations.

2.2.1 Bistable Configuration under Sinusoidal Excitations

In this section, the gap between the repulsive magnets is fixed at D=8.5mm. Firstly,

for different excitation levels, the dynamics of this bistable configuration in terms of open circuit voltage output under sinusoidal excitation (12Hz) is investigated, as shown in Figure 9. Given low-level excitations (a_{RMS}=1m/s^2), initial small-amplitude oscillation is observed (Figure 9(a)). With a disturbance applied (Throughout this paper, the disturbance mentioned is applied manually by using a small plastic hammer in the experiment), oscillations with larger amplitude are achieved. These oscillations, however, are still confined in one potential well (also observed in the experiment). Such oscillation is termed as "small limit cycle oscillation" (or "small LCO" in short). In Figure 9(b), the excitation level increases to a_{RMS}=1.4m/s^2, but it is still not strong enough to drive the harvester to jump between the two potential wells. Even with a disturbance applied, the harvester restores the small LCO around one of the two stable equilibriums after some transients. With further increase of a_{RMS} (Figure 9(c)), the harvester can be driven to jump between two potential wells by disturbance. Such large-amplitude oscillation is termed "large limit cycle oscillation" (or "large LCO" in short). Under significantly large excitations, chaotic oscillations are initially captured and then followed by large LCO with some disturbance (Figure 9(d)), or even without disturbance (Figure 9(e)).

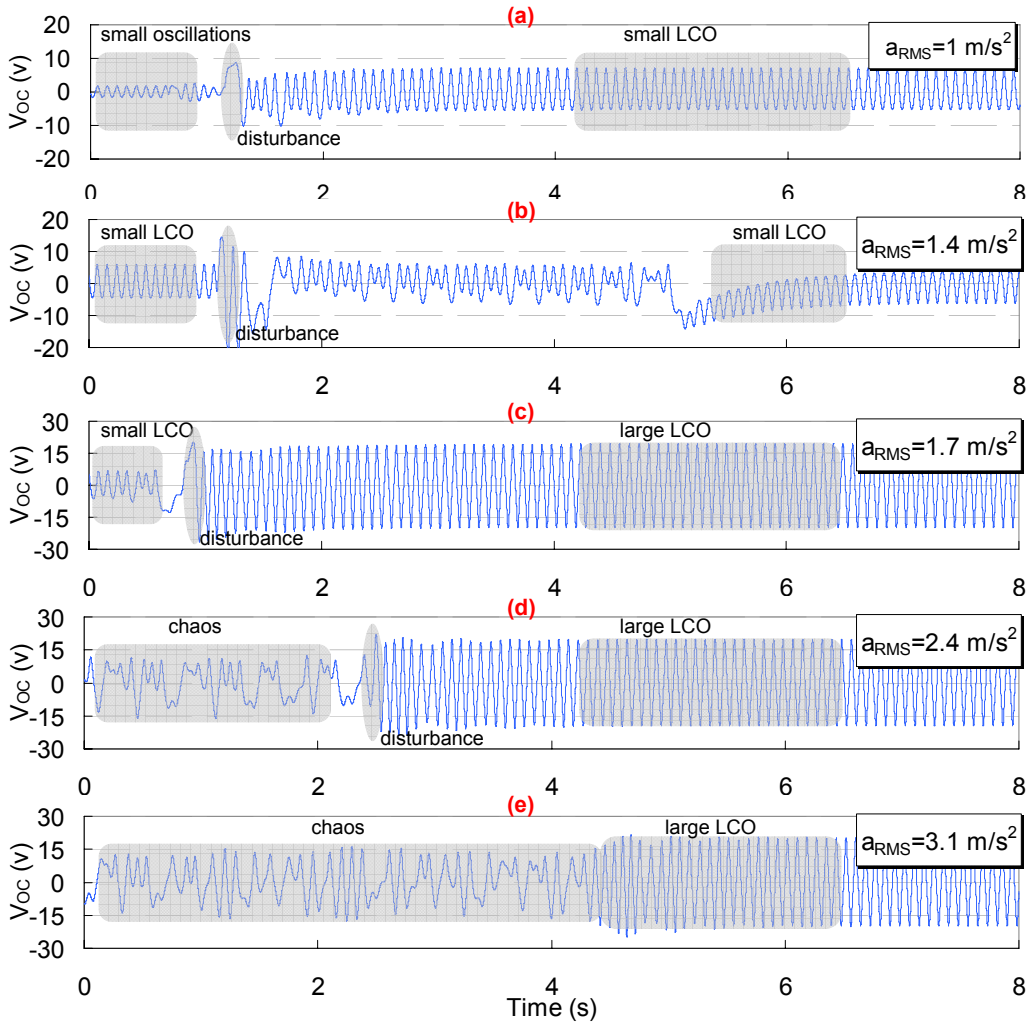

Figure 9 Dynamics of a bistable configuration under sinusoidal excitations (12Hz)

Obviously, if the large LCO can be captured and maintained at various frequencies, the bistable nonlinear energy harvester will be more efficient and functional. Figure 10 shows the sinusoidal upward sweep responses of the bistable and linear configurations with different excitation levels. The solid line depicts the performance of the bistable harvester by upward sweep without any disturbance applied. When disturbances are applied during upward sweep, multi-value response may exist. The dashed line depicts the maximum response achievable at each frequency, which can

be regarded as the best performance of the bistable harvester. Under low-level excitations (a_{RMS}=0.7m/s^2, Figure 10(a)), an important finding is that the response has the same pattern as that of monostable softening harvester (Figure 4(b)). The small LCO is captured by disturbance. With increased excitation level (a_{RMS}=1.4m/s^2), the large LCO is firstly captured in low-frequency range (7Hz~10Hz) by disturbance. With further increase in the excitation level (a_{RMS}=2.1m/s^2, Figure 10(c)), not only the frequency range for large LCO is extended (7Hz~16Hz), but also the small LCO is captured by disturbance in high-frequency range (22Hz~24Hz). In addition, within certain range (12Hz~14Hz), either small oscillation or small LCO or large LCO can occur depending on whether and how the disturbance is applied. Under strong excitations (a_{RMS}=2.8m/s^2), the response is similar to Figure 10(c) except that in some ranges, the bistable harvester captures frequency-lowered large LCO with disturbance (17Hz~19Hz) or chaotic oscillations (10Hz~14Hz).

In addition, the maximum responses (large LCO captured) of the bistable harvester are comparable with those of the linear configuration (Figures 10(b) to 10(d)). On the other hand, if the large LCO is maintained, wider bandwidth is achieved and it increases with the excitation level. Thus, bistable configuration is definitely able to improve the performance of the harvester. However, under practical random excitations, the large LCO may not be captured and maintained. This is because the probability for the harvester to jump between two potential wells depends on the energy barrier δ (Figure 3). If the small LCO or chaotic oscillations are captured, due

to their smaller magnitudes compared to the linear configuration, the bistable configuration may not be able to warrant better performance.

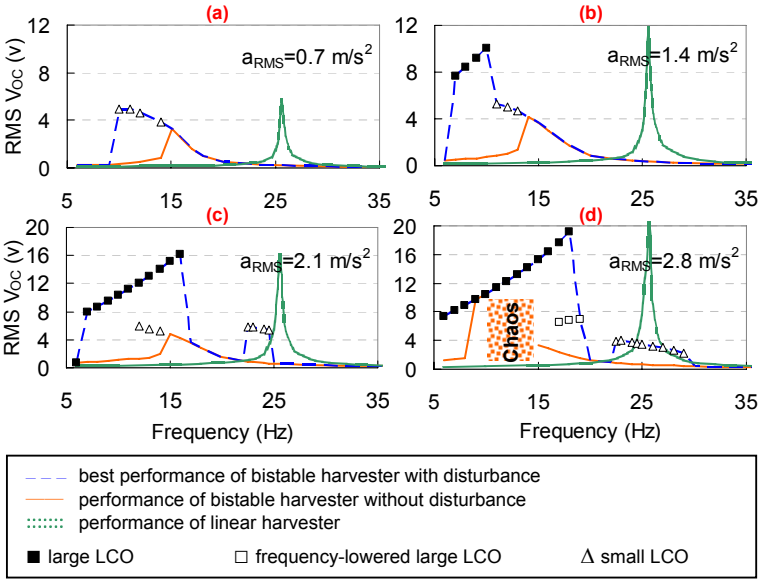

Figure 10 Sinusoidal sweep responses of bistable configurations versus linear configuration for various excitation levels

2.2.2 Bistable Configuration under Random Excitations

The V_{OC} responses in time domain for various bistable and linear configurations, under three different levels of random excitations, are compared in Figure 11. When the repulsive magnets are placed at D=9mm, due to the two close and shallow potential wells separated by a low energy barrier δ, the bistable harvester can easily jump between the potential wells and capture the large LCO at all three excitation levels. Thus the bistable configuration provides much larger voltage responses than the linear configuration, as compared in Figures 11(a) to (f). Reducing D between the repulsive magnets separates further the two potential wells but meanwhile increases

the energy barrier δ (Figure 3). Therefore, the probability for the harvester to jump between two potential wells under random excitations will be reduced. For D=8.5mm, only 2~3 jumps are observed (Figure 11(g)) under low-level excitations (a_{RMS}=2.5m/s^2), and the large LCO can be captured under larger excitations (Figures 11(h) to 11(i)). For D=8.2mm, under low-level excitations (a_{RMS}=2.5m/s^2), oscillations are totally confined in one potential well (Figure 11(j)) and the magnitude is much smaller compared to Figure 11(d). When the excitation level increases to 5m/s^2, only a few jumps appear (Figure 11(k)). When the excitation level further increases to 10m/s^2, frequent jumps are observed (Figure 11(l)), implying that the large LCO is captured. With further decrease of the gap (D=8mm), only infrequent jumps occur even though a_{RMS} is increased to 10m/s^2. Once the oscillations are confined in one potential well, there will be no guarantee that the bistable configuration will outperform the linear one.

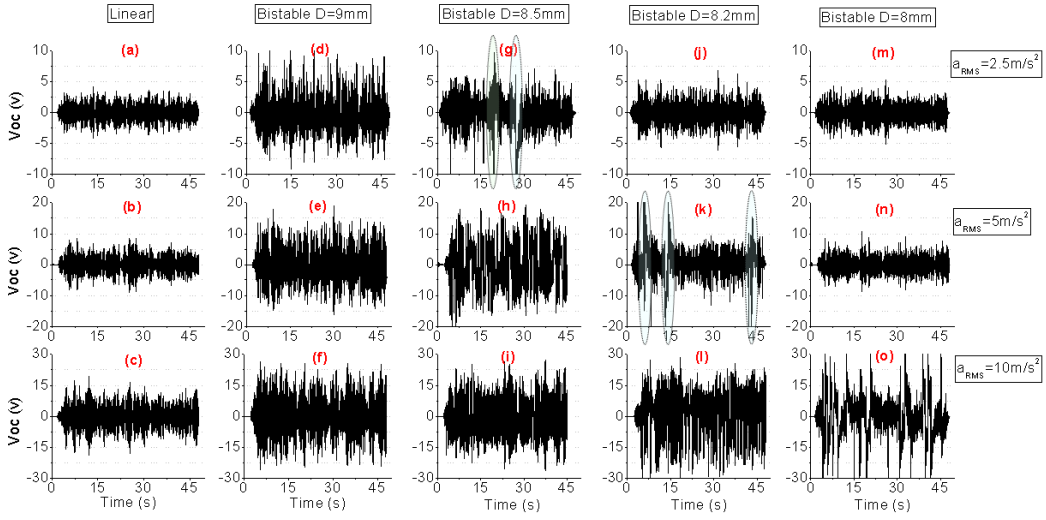

Figure 11 V_{OC} of linear and bistable configurations under random excitations. The eclipses in (g) and (k) highlight the infrequent jumps between the two potential wells.

To further evaluate the performance of various bistable configurations, an energy storage circuit is connected to the harvester to charge the 33μF capacitor. The voltage developed across the capacitor for various configurations and excitation levels is compared in Figure 12. It is observed that the bistable configurations outperform the linear configuration at all three excitation levels except for D=8mm, in which case the increased energy barrier firmly confines the harvester to oscillate in one potential well, thus deteriorating its performance. Besides, it is observed that when D=9mm, the harvester achieves the best performance of all three excitation levels. In addition, at high excitation level (a_{RMS}=10m/s^2) and except for D=8mm, there is no significant difference in the performance of bistable configurations due to the fact that the large LCO is captured when D=9, 8.5 and 8.2mm. These results are consistent with the observation of V_{OC} in Figure 11.

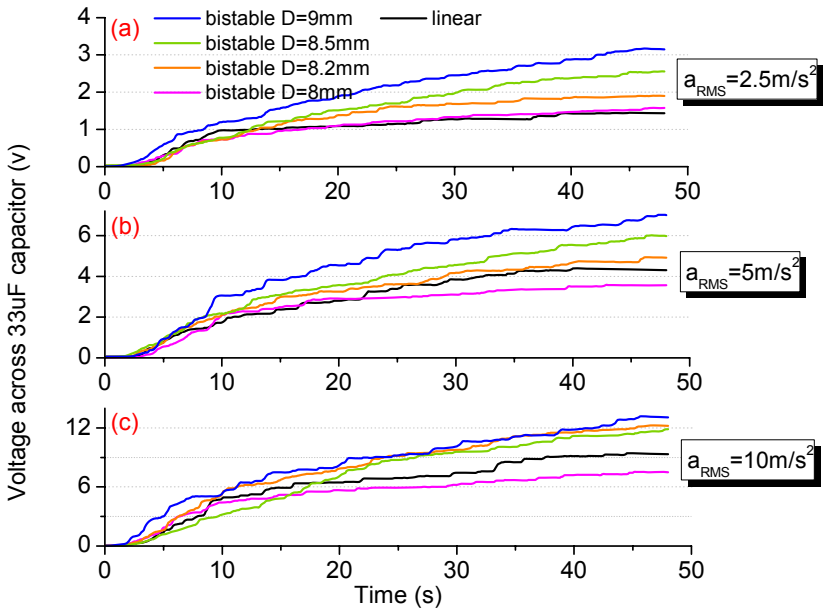

Figure 12 Voltage developed across storage capacitor for linear and bistable

configurations under random excitations

To investigate the bandwidth of bistable configurations under random excitations, fast Fourier transform (FFT) is conducted on the V_{OC} signal shown in Figure 11. The results are shown in Figure 13. Under low-level excitations (a_{RMS}=2.5m/s^2), since the oscillations of the bistable harvester are mostly confined in one potential well, obvious peaks appear in the V_{OC} spectra, especially for D=8.2 and 8mm.These peaks correspond to the post-buckled fundamental resonance frequency of the cantilever beam (Erturk et al., 2009). For D=8.5mm, the peak is not obvious and the V_{OC} amplitude is significantly increased at low frequency range due to the infrequent jumps between two potential wells (Figure 11(g)). For D=9mm, the useful bandwidth is obtained at low frequency range and the V_{OC} amplitude is much larger than the other configurations because the large LCO can always be captured. When the excitation level increases, the peaks in the spectra of bistable configurations disappear, indicating that the oscillations of the harvester are dominated by the large LCO. For example, for D=8.5mm, a flat peak exists when a_{RMS}=2.5m/s^2 but disappears when a_{RMS}=5 and 10m/s^2. Besides, under high-level excitations (a_{RMS}=10m/s^2), the V_{OC} magnitude of linear configuration in the frequency domain is comparable with those of bistable configurations (D=9, 8.5, 8.2mm) (Figure 13(c)). However, similar to the discussion in Section 2.1.2, the significantly increased bandwidth of the bistable configurations (e.g., D=9mm) results in the increased V_{OC} outputs in the time domain (e.g., Figures 11(f), 11(i) and 11(l)) and thus the advantageous performance for

charging the capacitor over the linear configuration (Figure 12(c)). The observation that the bandwidth increases with the excitation level is consistent with the best performances shown in Figures 10(b) to 10(d). In addition, the V_{OC} spectra for D=9, 8.5 and 8.2mm almost overlap (Figure 13(c)), which explains why the performances of these configurations are almost the same (Figure 12(c)).

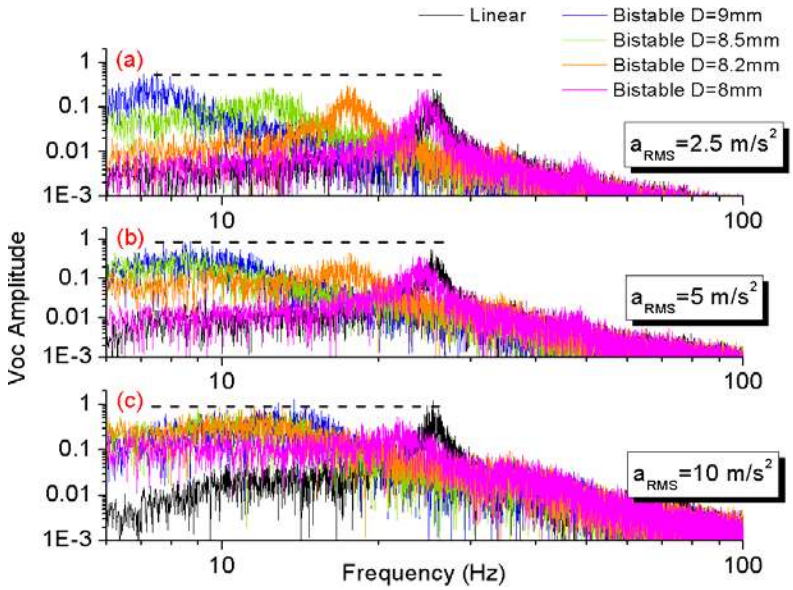

Figure 13 V_{OC} spectra (FFT) of linear and bistable configurations under random excitations

2.2.3 Summary of Bistable Configuration

A bistable nonlinear energy harvester can be implemented using repulsive magnets. Under low-level sinusoidal excitations, the oscillations of the bistable harvester are confined in one potential well and its frequency sweep response shows the same pattern as that of a monostable softening configuration. Under high-level sinusoidal excitations, oscillations of different types, including small oscillation, small LCO, large LCO, frequency-lowered large LCO and chaotic oscillation, can show up with

proper disturbance. Once the large LCO is captured, useful wider bandwidth can be achieved compared to the linear configuration. Under practical broadband random excitations, the bistable configuration is demonstrated to always be capable of outperforming the linear configuration except when the repulsive magnets are too closely placed, in which case oscillations are mostly confined in one potential well. With a large gap D between the magnets (D=9mm), the large LCO can always be captured and the harvester performs best at various excitation levels. Similar to the monostable configuration, the improved performance of a bistable configuration can be attributed to two aspects: the increased output magnitude in the frequency domain for low-level excitations and the significantly enlarged bandwidth for high-level excitations.

2.3 Optimal Nonlinear Configuration

Reducing the gap D between two repulsive magnets can change a nonlinear harvester from a monostable configuration to a bistable configuration. Figure 7 in Section 2.1 shows that the performance of a monostable hardening configuration increases when D decreases. While, in Section 2.2, Figure 12 indicates that generally, the performance of a bistable configuration declines when D decreases. These results suggest that the optimal performance of nonlinear configuration could be achieved around the region where a monostable configuration transforms into a bistable one (i.e., D approaches D*).

To verify the above conjecture, Figure 14 compares the energy accumulated in the storage capacitor within 45 seconds for various nonlinear configurations under random excitations. Although the energy accumulated for each case is not exactly repeatable due to the nature of random excitations, the tendency in Figure 14 is clear, that is, the optimal performance of nonlinear configuration at various excitation levels is achieved around the monostable-to-bistable transition region. This important finding reveals two anti-intuitive facts: (1) Not only bistable but also monostable configuration can achieve optimal performance, when their repulsive magnets are arranged close to the monostable-to-bistable transition region, though the bistable configuration has been more enthusiastically pursued and reported in the literature due to its larger bandwidth (we can see this when comparing Figure 8(c) and Figure 13(c)); and (2) It is unnecessary to design a bistable energy harvester with two potential wells separated far away. Intuitively, by reducing D, larger voltage output is expected when the harvester oscillates between further separated potential wells. However, certain mechanism such as exploiting stochastic resonance (McInnes et al., 2008) should be implemented to overcome the high energy barrier, which not only induces the complexity in harvester design but also consumes some amount of the harvested energy. Fortunately, the findings in this study show that a bistable configuration with large D (meaning shallow potential wells separated by low energy barrier) close to the monostable-to-bistable transition region will provide better performance (Figure 14). Thus, we can avoid the high energy barrier issue. These results provide important guidelines for designing a nonlinear energy harvester.

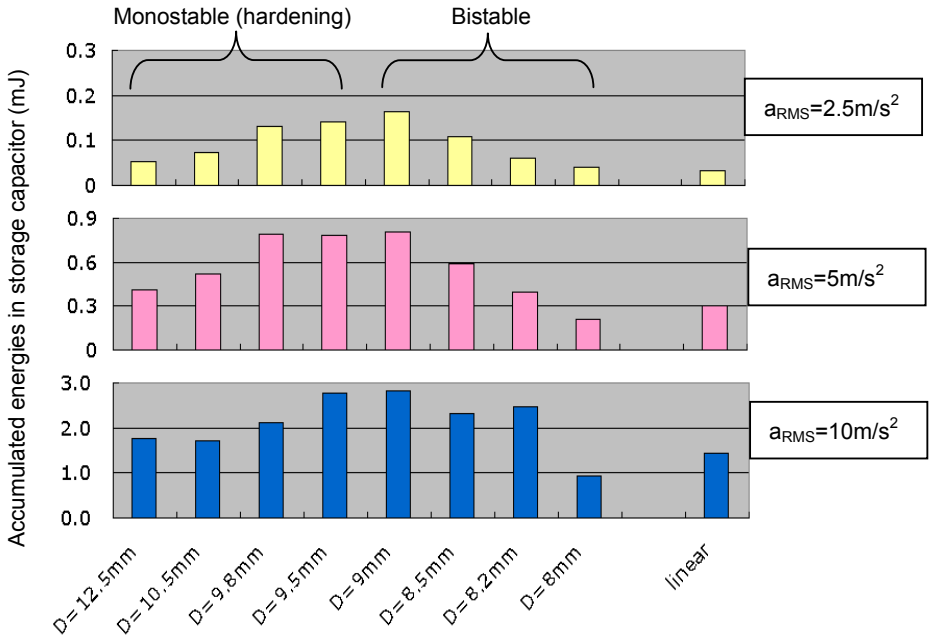

Figure 14 Accumulated energies in storage capacitor with various configurations

3 FREQUENCY UP-CONVERSION USING MAGNETS

In some ultra-low-frequency vibration scenarios such as human movements (~1Hz) and wave heave motions (<1Hz), tuning resonance or exploiting nonlinearity is obviously infeasible. Hence, in these scenarios, certain frequency up-conversion mechanism should be implemented to improve the functionality of the energy harvesters. Pairs of magnets (Rastegar and Murray (2009)) or ferromagnetic structures (Wickenheiser and Garcia (2010)) can be exerted in frequency up-conversion mechanism. However, according to the literature, only attractive magnetic forces have been considered so far. In this section, both repulsive and attractive magnetic configurations for frequency up-conversion are investigated. Wave heave motion is taken as an example of low-frequency vibration source and parametric study is

performed to compare the efficiency of various configurations under various wave conditions.

3.1 Frequency Up-Conversion Mechanism

The proposed frequency up-conversion mechanism, using both repulsive and attractive magnets, is illustrated in Figure 15(a). The piezoelectric bimorph cantilever is the same as that used in the frequency tuning or nonlinear energy harvester configuration for vibration-to-electricity transduction. However, the difference between them is the way excitations are applied. In the nonlinear energy harvester configurations, piezoelectric cantilever and magnets are applied with base excitations as a whole. While, in the frequency up-conversion mechanism, the piezoelectric cantilever stands still and is excited by magnetic force applied at the free end. The magnet, which follows motions from the low-frequency vibration source, regularly passes by and interacts with another magnet fixed at the free end of the piezoelectric cantilever and thus excites the cantilever to vibrate at its high natural frequency. Buoy-based sensors can be powered by efficient wave energy harvester using such frequency-up conversion mechanism as shown in Figure 16. The experimental implementation of frequency up-conversion is shown in Figure 15(b). The cantilever is clamped and stands still at the rim of the shaker, and one magnet is fixed at the shaker shaft undergoing low-frequency sinusoidal motions to mimic wave heave motions. Since significant noise appears in the signals of the accelerometer under ultra-low-frequency vibrations, the magnitude of motion generated by the shaker is

directly recorded by a pen. In later sections, parametric study is conducted to compare the efficiency of various repulsive and attractive magnetic configurations under various wave conditions.

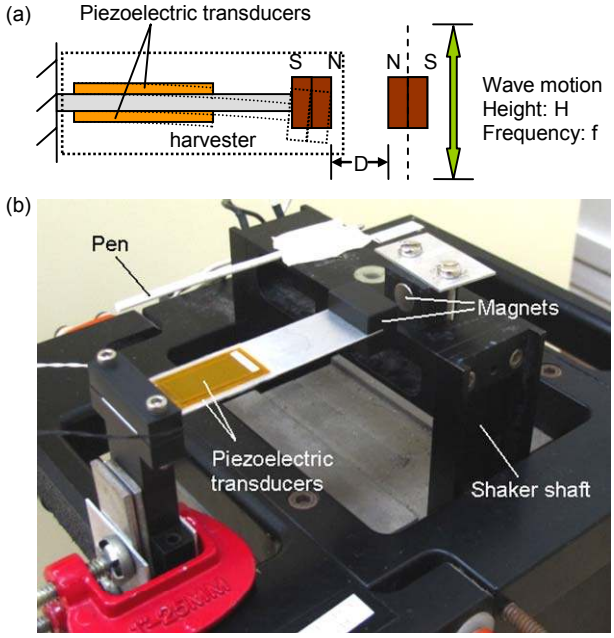

Figure 15 Frequency up-conversion mechanism and experimental implementation

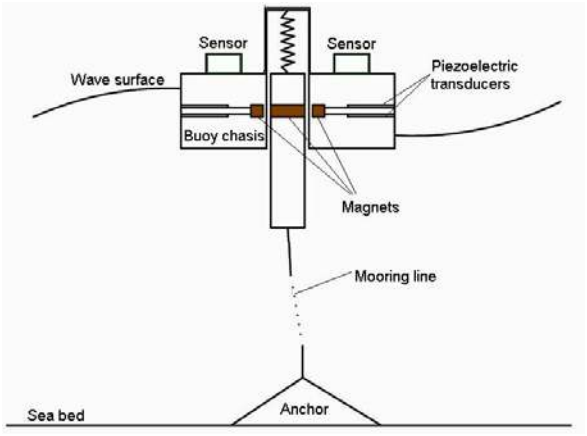

Figure 16 Conceptual drawing of buoy-based sensors powered by wave energy harvester using frequency up-conversion technique

3.2 Repulsive Magnets for Frequency Up-Conversion

The repulsive magnetic configuration is first investigated. The gap between the repulsive magnets is set to be D=12mm, 8mm and 6mm, respectively. For each case, the performance of the harvester is studied for three wave heights H=15mm, 30mm and 50mm, and three frequencies f=0.4Hz, 0.6Hz and 0.8Hz.

For a large gap between the repulsive magnets (D=12mm), the open circuit voltage V_{OC} under various wave conditions is shown in Figure 17. It can be observed that the harvester is not effectively excited by the weak magnetic forces. Here, "effectively excited" refers to that the piezoelectric cantilever is excited to vibrate at its high natural frequency. For lower H and f, the deflection of the harvester just follows the wave heave motion. With the increase of H and f, the excited high-frequency vibrations appear, though the magnitude is small, as shown in Figures 17(h) and 17(i). When the energy storage circuit is connected, the voltage developed across the 33μF capacitor is as illustrated in Figure 18. It is noted that generally, the energy accumulation is very slow for D=12mm. The energy harvesting performance is improved with the increase of H and f, in accordance with the observations of V_{OC}.

For a medium gap between the repulsive magnets (D=8mm), V_{OC} under different wave conditions is shown in Figure 19. In this case, the piezoelectric cantilever is effectively excited and experiences quasi damped free vibrations between two impulses induced by magnetic forces. Substantial increase in the magnitude of V_{OC} is

observed as compared to Figure 17. The significant efficiency improvement is also reflected in the voltage developed when the harvester charges the storage capacitor (Figure 20). However, the performance is still sensitive to the wave conditions. More vigorous wave motions (larger H and f) generate more electricity, as shown in Figure 20.

With further decrease of the gap (D=6mm), no matter under which wave condition, the piezoelectric cantilever can be effectively excited and the peak-to-peak magnitude of V_{OC} after one impulse is around 45V, as shown in Figure 21. The only difference is that the excited large-magnitude output is divided into different number of segments for different wave frequency. Considering the energy storage circuit, Figure 22 clearly shows that when the repulsive magnets are sufficiently close (D=6mm), the energy harvested is relatively insensitive to the wave conditions (H and f). This characteristic is preferable for wave energy harvesting in the uncertain marine environment. Besides, for D=6mm, the energy harvesting capability approaches saturation. For instance, under wave motion of H=50mm and f=0.8Hz, only 3V (~20%) increase is observed in the voltage developed across the 33μF capacitor for 45 seconds, as compared to that for D=8mm (Figure 22(c) and Figure 20(c)).

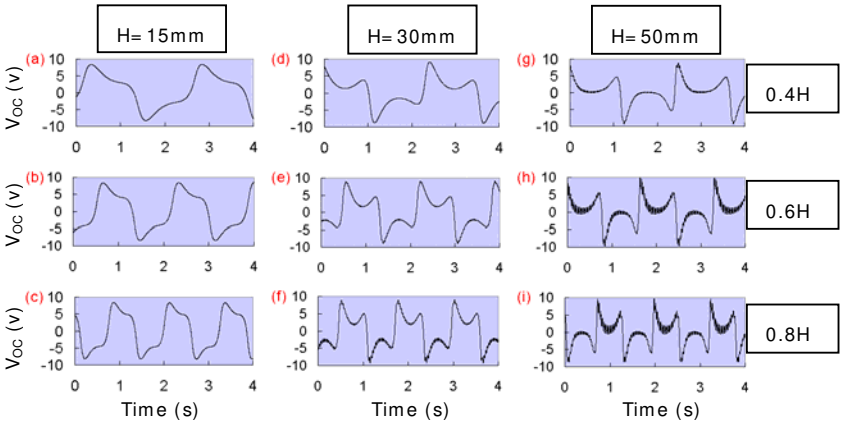

Figure 17 V_{OC} for different H and f. Repulsive magnets with D=12mm

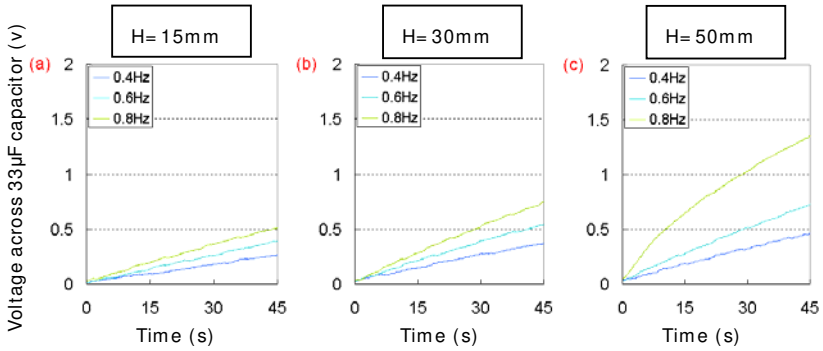

Figure 18 Voltage across storage capacitor for different H and f. Repulsive magnets with D=12mm

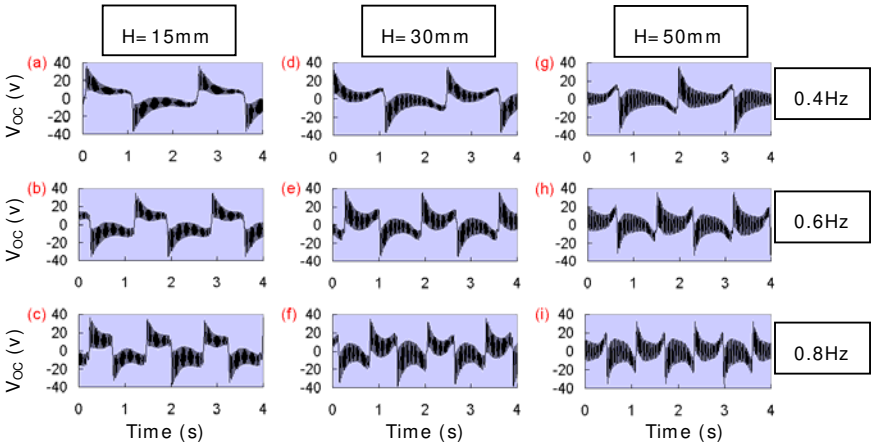

Figure 19 V_{OC} for different H and f. Repulsive magnets with D=8mm

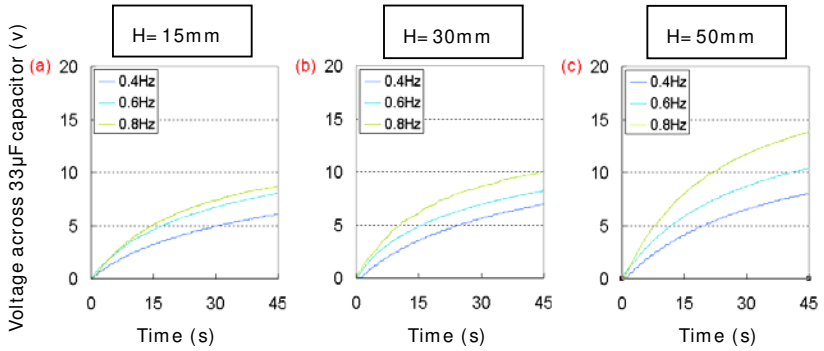

Figure 20 Voltage across storage capacitor for different H and f. Repulsive magnets with D=8mm

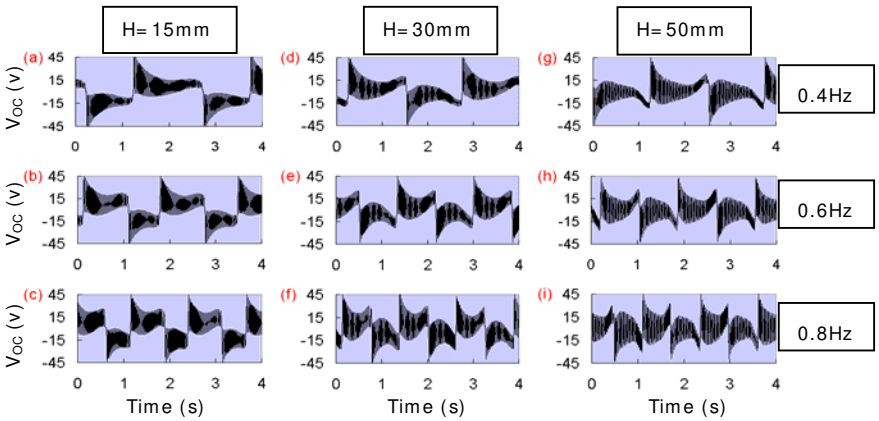

Figure 21 V_{OC} for different H and f. Repulsive magnets with D=6mm

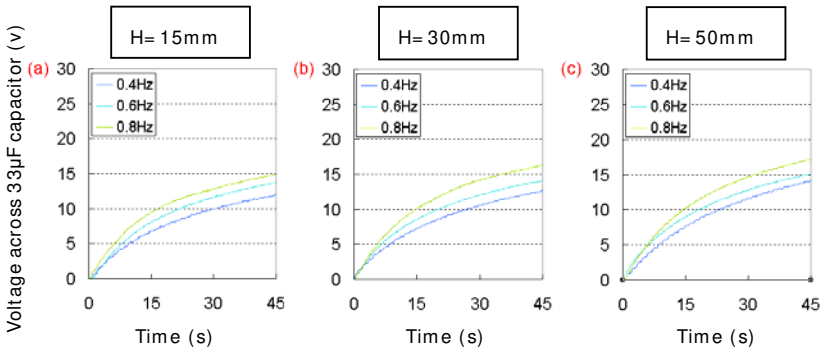

Figure 22 Voltage across storage capacitor for different H and f. Repulsive magnets with D=6mm

3.3 Attractive Magnets for Frequency Up-Conversion

Attractive magnetic configuration is also investigated for frequency up-conversion mechanism to compare with the repulsive configuration. For a large gap between the attractive magnets (D=12mm), it is observed in Figure 23 that no matter under which wave condition, the harvester just follows the heave motion rather than vibrates at its natural frequency. Even though the gap is decreased to D=6mm, the harvester is still unable to be effectively excited by the attractive magnetic forces (Figure 24). The high-frequency vibrations of the harvester only appear under extremely vigorous wave motion (H=50mm, f=0.8Hz, Figure 24(d)). However, compared to the repulsive case (Figure 21(i)), the magnitude of the excited high-frequency vibrations and thus the energy harvesting efficiency by attractive configuration is drastically lower. Hence, given same parameters and wave conditions, the repulsive magnetic configuration is preferable in frequency up-conversion mechanism.

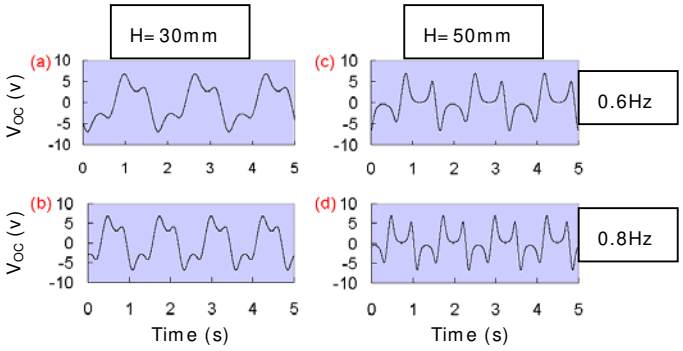

Figure 23 V_{OC} for different H and f. Attractive magnets with D=12mm

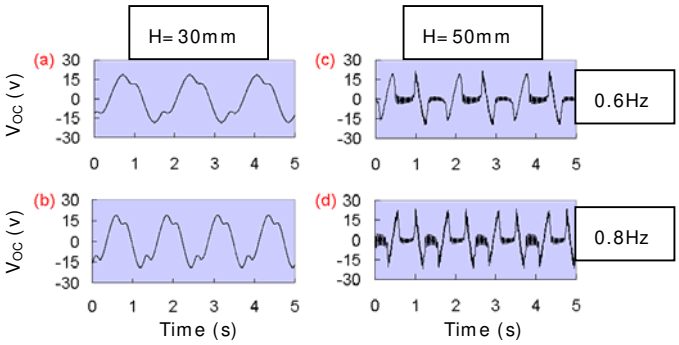

Figure 24 V_{OC} for different H and f. Attractive magnets with D=6mm

4 CONCLUSIONS

This paper presents our experimental investigation on the merits of using magnets to improve the functionality of vibration energy harvesters under various scenarios. The nonlinearities introduced by magnets and the frequency up-conversion technique using magnets have been given the most attention. Main findings of this work can be summarized as follows:

Exploiting nonlinearities using magnets

- Monostable configuration. Under low-level sinusoidal excitations, the nonlinear part of the magnetic force is negligible, while the linear part of the magnetic force contributes to changing the stiffness of the harvester and thus can be used for resonance tuning. Under high-level sinusoidal excitations, high-energy and low-energy orbits co-exist in certain frequency range. Wider bandwidth for efficient energy harvesting can be achieved by proper sweep or by disturbance especially for monostable hardening configurations. Under practical random excitations, monostable hardening configuration can significantly outperform the

linear configuration, especially when the repulsive magnets are closely placed (D=9.5mm). The improved performance can be attributed to two aspects: the increased output magnitude in the frequency domain for low-level excitations and the enlarged bandwidth for high-level excitations.

- Bistable configuration. Under low-level sinusoidal excitations, oscillations of a bistable configuration may be confined in one potential well and the frequency sweep response shows the same pattern as that of a monostable softening configuration. Under high-level sinusoidal excitations, oscillations of different types, including small oscillation, small LCO, large LCO, frequency-lowered large LCO and chaotic oscillations can show up with proper disturbance. Once the large LCO is captured, useful wider bandwidth can be achieved as compared to the linear configuration. Under practical random excitations, bistable configurations can always outperform the linear configuration except when the repulsive magnets are too closely placed, in which case, oscillations of the harvester are firmly confined in one potential well. For a large gap between the magnets (D=9mm) at various excitation levels, the large LCO is always easily captured, which gives the best performance among all bistable configurations. In addition, similar to monostable configuration, the improved performance of bistable configuration can be attributed to two aspects: the increased output magnitude in the frequency domain for low-level excitations and the significantly enlarged bandwidth for high-level excitations.
- Optimal nonlinear configuration. The configuration for optimal performance of a

nonlinear energy harvester is found near the monostable-to-bistable transition region (i.e., D≈D*). This is an important finding in this work which tells us two anti-intuitive things: (1) Not only bistable but also monostable configurations can achieve optimal performance when their repulsive magnets are arranged close to the monostable-to-bistable transition region; and (2) It is unnecessary to design a bistable energy harvester with two potential wells separated far away. A bistable configuration with larger D close to the monostable-to-bistable transition region can provide better performance. Thus, we can also avoid the difficulty in implementing certain mechanism such as exploiting stochastic resonance (McInnes et al., 2008) to overcome the high energy barrier issue.

Frequency up-conversion using magnets

- In ultra-low-frequency vibration scenarios, such as wave heave motions, the frequency up-conversion technique using magnets is proposed. Different configurations under various wave conditions are investigated by parametric study. The repulsive configuration of magnets is found preferable in the frequency up-conversion technique, which can efficiently excite the cantilevered energy harvester to vibrate at its high fundamental natural frequency. When the repulsive magnets are placed sufficiently close, the energy harvesting capability can be saturated and relatively insensitive to various wave conditions. Hence, the energy harvester can be functional and adaptive in the uncertain marine environment.

The findings presented in this paper serve as useful design guidelines when one seeks nonlinearity or frequency up-conversion techniques using magnets to improve the functionality of vibration energy harvesters.

REFERENCES

Andò, B., Baglio, S., Trigona, C., Dumas, N., Latorre, L. and Nouet, P. 2010. "Nonlinear Mechanism in MEMS Devices for Energy Harvesting Applications," *J. Micromech. Microeng.*, 20:125020.

Anton, S.R. and Sodano, H.A. 2007. "A Review of Power Harvesting Using Piezoelectric Materials (2003-2006)," *Smart Mater. and Struct.*, 16:R1-R21.

Bracewell, R.N. 1978. "Rayleigh's Theorem," *The Fourier Transform and Its Applications*, *2nd Edition*, McGraw-Hill, pp.112-113.

Challa, V.R., Prasad, M.G. and Fisher, F.T. 2011. "Towards An Autonomous Self-Tuning Vibration Energy Harvesting Device for Wireless Sensor Network Applications," *Smart Mater. Struct.*, 20: 025004.

Challa, V.R., Prasad, M.G., Shi, Y. and Fisher, F.T. 2008. "A Vibration Energy Harvesting Device with Bidirectional Resonance Frequency Tunability," *Smart Mater. Struct.*, 17:015035.

Cottone, F., Vocca, H. and Gammaitoni, L. 2009. "Nonlinear Energy Harvesting." *Phys. Rev. Lett.*, 102: 080601.

Daqaq, M.F. 2010. "Response of Uni-Modal Duffing-Type Harvesters to Random Forced Excitations," *J. Sound Vib.*, 329:3621–3631.

El-Hami, M., Glynne-Jones, P., White, N.M., Beeby, S., James, E., Brown, A.D. and Ross, J.N. 2001. “Design and Fabrication of A New Vibration-Based Electromechanical Power Generator,” *Sens. Actuat. A*, 92:335-342.

Erturk, A., Hoffmann, J. and Inman, D.J. 2009. “A Piezomagnetoelastic Structure for Broadband Vibration Energy Harvesting,” *Appl. Phys. Lett.*, 94:254102.

Ferrari, M., Ferrari, V., Guizzetti, M., Andò, B., Baglio, S. and Trigona, C. 2010. “Improved Energy Harvesting from Wideband Vibrations by Nonlinear Piezoelectric Converters,” *Sens. Actuat. A*, 162:425-431.

Formosa F., Büssing T., Badel A. and Marteau, S. 2009. “Energy Harvesting Device with Enlarged Frequency Bandwidth Based on Stochastic Resonance”, *Proceedings of PowerMEMS 2009*, Washington D.C., USA, pp.229-232.

Hu, Y., Xue, H. and Hu, H. 2007. “A Piezoelectric Power Harvester with Adjustable Frequency through Axial Preloads,” *Smart Mater. Struct.*, 16:1961-1966.

Leland, E.S. and Wright, P.K. 2006. “Resonance Tuning of Piezoelectric Vibration Energy Scavenging Generators Using Compressive Axial Preload,” *Smart Mater. Struct.*, 15:1413-1420.

Lin, J. and Alphenaar, B. 2010. “Enhancement of Energy Harvested from a Random Vibration Source by Magnetic Coupling of a Piezoelectric Cantilever,” *J. Intell. Mater. Syst. Struct.*, 21(13):1337-1341.

Mann, B.P. and Sims, N.D. 2009. “Energy Harvesting from The Nonlinear Oscillations of Magnetic Levitation,” *J. Sound Vib.*, 319:515-530.

McInnes, C.R., Gorman, D.G. and Cartmell, M.P. 2008. “Enhanced Vibrational Energy

Harvesting Using Nonlinear Stochastic Resonance," *J. Sound Vib.*, 318:655-662.

Peters, C., Maurath, D., Schock, W., Mezger, F. and Manoli, Y. 2009. "A Closed-Loop Wide-Range Tunable Mechanical Resonator for Energy Harvesting Systems," *J. Micromech. Microeng.*, 19:094004.

Ramlan, R., Brennan, M.J., Mace, B.R. and Kovacic, I. 2010. "Potential Benefits of A Non-linear Stiffness in An Energy Harvesting Device," *Nonlinear Dynamics*, 59:545-558.

Rastegar, J. and Murray, R. 2009. "Novel Two-Stage Piezoelectric-Based Electrical Energy Generators for Low and Variable Speed Rotary Machinery," *Proceedings of SPIE*, 7288:72880B.

Rastegar, J., Pereira, C. and Nguyen, H-L. 2006. "Piezoelectric-Based Power Sources for Harvesting Energy from Platforms with Low-Frequency Vibration," *Proceedings of SPIE*, 6171:617101.

Roundy, S., Wright, P.K. and Rabaey, J. 2003. "A Study of Low Level Vibrations as A Power Source for Wireless Sensor Nodes," *Computer Communications*, 26:1131-1144.

Stanton, S.C., McGehee, C.C. and Mann, B.P. 2009. "Reversible Hysteresis for Broadband Magnetopiezoelastic Energy Harvesting," *Appl. Phys. Lett.*, 95:174103.

Stanton, S.C., McGehee, C.C. and Mann, B.P. 2010. "Nonlinear Dynamics for Broadband Energy Harvesting: Investigation of A Bistable Piezoelectric Inertial Generator," *Physica D*, 239:640-653.

Tang, L.H. and Yang, Y.W. 2011. "Analysis of Synchronized Charge Extraction for Piezoelectric Energy Harvesting," *Smart Mater. Struct.*, 20: 085022.

Tang, L.H., Yang, Y.W. and Soh, C.K. 2010. "Towards Broadband Vibration-Based Energy

Harvesting," *J. Intell. Mater. Syst. Struct.*, 21(18):1867-1897.

Wang, L. and Yuan, F.G. 2008. "Vibration Energy Harvesting by Magnetostrictive Material," *Smart Mater. Struct.*, 17:045009.

Wickenheiser, A.M. and Garcia, E. 2010. "Broadband Vibration-Based Energy Harvesting Improvement through Frequency Up-Conversion by Magnetic Excitation," *Smart Mater. Struct.*, 19:065020.

Wischke, M., Masur, M., Goldschmidtboeing, F. and Woias, P. 2010. "Electromagnetic Vibration Harvester with Piezoelectrically Tunable Resonance Frequency," *J. Micromech. Microeng.*, 20:035025.

Yang, Y.W. and Tang, L.H. 2009. "Equivalent Circuit Modeling of Piezoelectric Energy Harvesters", *J. Intell. Mater. Syst. Struct.*, 20:2223-2235.

Yang, Y.W., Tang, L.H. and Li, H.Y. 2009. "Vibration Energy Harvesting Using Macro-Fiber Composites," *Smart Mater. Struct.*, 18:115025.